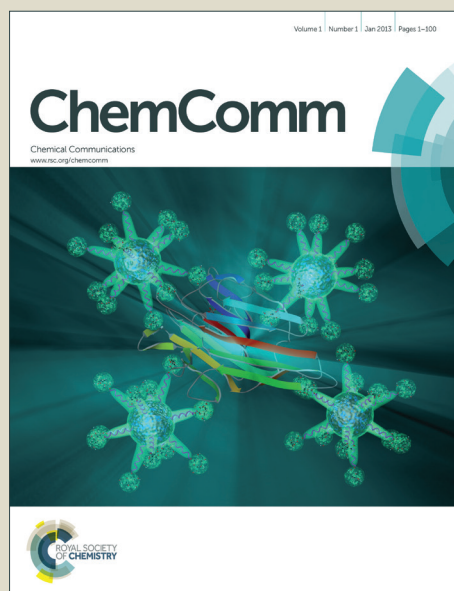


ChemComm

Accepted Manuscript



This is an *Accepted Manuscript*, which has been through the Royal Society of Chemistry peer review process and has been accepted for publication.

Accepted Manuscripts are published online shortly after acceptance, before technical editing, formatting and proof reading. Using this free service, authors can make their results available to the community, in citable form, before we publish the edited article. We will replace this *Accepted Manuscript* with the edited and formatted *Advance Article* as soon as it is available.

You can find more information about *Accepted Manuscripts* in the [Information for Authors](#).

Please note that technical editing may introduce minor changes to the text and/or graphics, which may alter content. The journal's standard [Terms & Conditions](#) and the [Ethical guidelines](#) still apply. In no event shall the Royal Society of Chemistry be held responsible for any errors or omissions in this *Accepted Manuscript* or any consequences arising from the use of any information it contains.

Chemical gardens without silica: The formation of pure metal hydroxide tubes

Received 00th January 20xx,
Accepted 00th January 20xx

Bruno C. Batista and Oliver Steinbock*

DOI: 10.1039/x0xx00000x

www.rsc.org/

Contrary to common belief, hollow precipitation tubes form in the absence of silicate if sodium hydroxide solution is injected into solutions of various metal ions. In many cases, the growth speed has a power law dependence on the flow rate. For vanadyl, we observe damped oscillations in the tube height.

The use of chemical reactions for the construction of non-crystalline macroscopic shapes appears to be an engineering feat that is mastered only by living systems.¹ However, certain non-biological chemical processes do self-organize complex structures that exceed typical molecular length-scales by many orders of magnitude.² Important examples for these nonequilibrium shapes and patterns include Turing patterns, chemical waves in reaction-diffusion media and specific precipitation structures that persist even after the system has reached equilibrium.³⁻⁵ Among the latter class of processes, the most iconic are silica or chemical gardens which consist of spontaneously forming hollow tubes reaching lengths of several centimeters.⁶

In the classical version of the silica garden experiment, a small salt particle is placed into a basic silicate solution.^{6,7} The dissolving salt induces the formation of metal hydroxide and silica. These products rapidly form a semi-permeable membrane around the seed and compartmentalize the system. Osmotic pressure then induces an influx of water and breaches the membrane to produce an osmotically driven, upward directed jet of slightly acidic salt solution.⁷ In the simplest case, the precipitation tube is templated around this jet and the jet's steep concentration gradients cause opposing concentration profiles in silica and metal hydroxide across the thin tube wall.⁸ Non-conventional examples of chemical gardens include tubes formed during the formation of polyoxometalates, rust, and cement.⁹

During the past decade the study of these structures has created the field of chemobrionics¹⁰ and expanded our

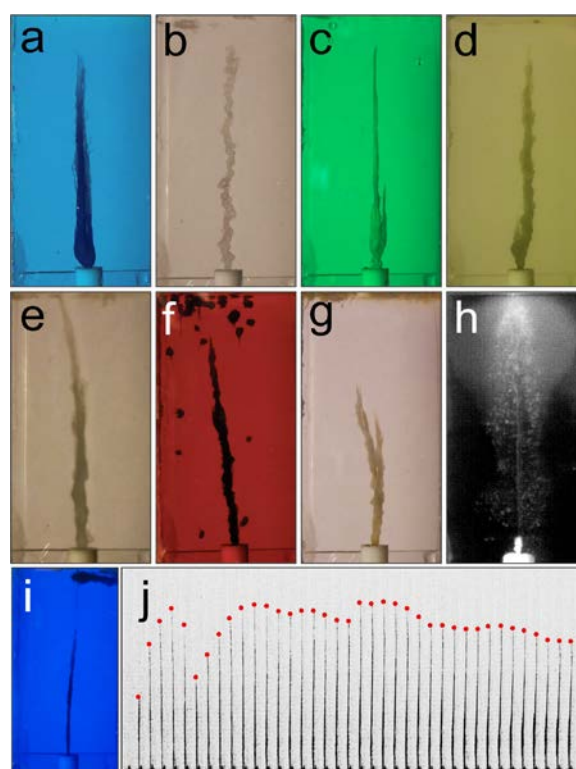


Fig 1. (a-i) Photographs of tubes growing during the injection of aqueous NaOH into solutions of the divalent cations Cu^{2+} , Zn^{2+} , Ni^{2+} , Fe^{2+} , Mg^{2+} , Co^{2+} , Mn^{2+} , Ca^{2+} , VO^{2+} , respectively. Pump rate is 8 mL/h and each frame is $3 \times 5.8 \text{ cm}^2$. (j) 40 min image sequence showing the growth and dissolution of $\text{VO}(\text{OH})_2$ tubes at a pump rate of 1 mL/h. Frame $1 \times 3.2 \text{ cm}^2$.

understanding of the tube materials and their potential applications as microchannels, luminescent devices, powerful Brønsted catalysts, and sensor platforms.¹¹⁻¹⁴ However, a quantitative description of the tubes' growth dynamics and often intricate morphology has been hindered by the complexity of the underlying physicochemical processes and the involvement of numerous reactants.^{6,7,15,16} In simple cases, these reactants are the metal ion, silicate (or comparable species such as phosphate or carbonate) as well as hydroxide and hydronium ions.^{6,7,16} We note that these four

^a Florida State University, Department of Chemistry and Biochemistry, Tallahassee, FL 32306-4390.

* Corresponding author. Email: steinbock@chem.fsu.edu

Electronic Supplementary Information (ESI) available: Raman spectra of powdered tubes, physicochemical properties of solutions, raw data of speeds and radii. Two movies showing the evolution of oscillatory (VO^{2+}) and fountain-like (Ca^{2+}) tube growth. See DOI: 10.1039/x0xx00000x

ions also have very different transport coefficients in the thickening tube wall, thus adding to the complexity of the problem. To overcome these complications we here describe conditions that involve a minimal set of reactants.

In our experiments, we inject sodium hydroxide solution (0.5 mol/L) into a large reservoir of metal salt solution (0.5 mol/L). The injection is carried out through a Teflon nozzle, at a constant flow rate, and in the upward direction. Figures 1a-i show representative tube structures grown in nine different divalent metal salt solutions (see caption). The images do *not* show pseudo-colors but rather represent the actual color of the salt solutions under transmitted white light. Especially at low pump rates, we occasionally observe branched tubes which are however rare or absent for cobalt, copper, and iron. Most tubes grow around a buoyant jet (not discernible in Fig. 1) indicating that the tube is open at its upper orifice.

The tube structures generated in our experiments are very fragile but increase in strength if the hydroxide solution is injected for several minutes. In the cases of iron, magnesium, and manganese chloride, tube segments can be readily extracted from the reactor. Tubes grown from copper chloride solution are the strongest and can be removed without breakage. Once the moist Cu, Co, Fe and Mn based structures are exposed to air, they readily change color.

Among the investigated compounds, our experiments show markedly different behavior for calcium chloride (h) and vanadyl sulfate solutions (i,j). For calcium, we observe a fountain-like ejection of colloidal particles and the slowest tube growth. The upward convecting particles also create a turbid cloud in the upper third of the reaction vessel (SI movie 1). For vanadyl, we find that low flow rates generate rhythmic dynamics with alternating phases of tube growth and tube dissolution. This behavior is illustrated in Fig. 1j, which is a collage of 20 subsequent image files (tube tip marked by a red dot), and SI movie 2. Tube growth followed by top-down dissolution is also observed for iron(III) chloride but the cycle does not repeat. We note that the latter solutions are the most acidic ones studied here.

All of the tubes shown in Fig. 1 are novel in the sense that they form in the absence of anions such as silicate and phosphate. We note, however, that Maselko et al. claimed the formation of metal hydroxide tubes in systems that contained high concentrations of carbonates.¹⁶ Unfortunately no materials analyses were presented. To ensure that the structures do not involve carbonates from atmospheric sources, all of our experiments were performed with nitrogen-purged solutions. In addition, we prepared all stock solutions with volumetric flasks made of polypropylene and no glass components were used in the experimental set-up. Accordingly, the synthesized tubes must consist—at least initially—of pure metal hydroxide. We note that the colors of the freshly formed samples are in agreement with this statement.

Figure 2 shows x-ray diffraction (XRD) patterns of eight different tube samples that were carefully filtrated in degassed water, dried anaerobically, and then transferred to the diffractometer under aerobic conditions (all at room temperature). The XRD patterns are sorted from top to bottom by decreasing signal-to-noise ratio. The data show clear indications of crystallinity for most samples, but

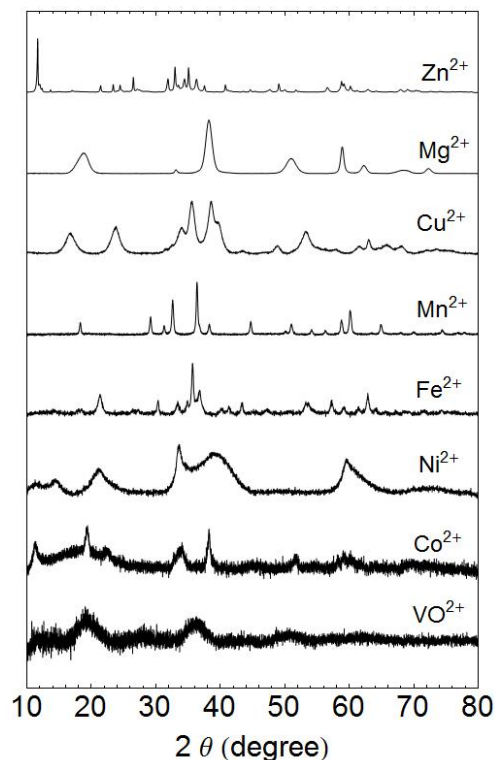


Fig 2. X-ray diffraction patterns of silica-free precipitation tubes. Samples of equal weight were collected from tubes grown at a pump rate of 8 mL/h. The concentration of OH⁻ and the divalent cations was 0.5 mol/L. All XRD signals were normalized to the same maximum intensity.

vanadyl, cobalt, and also nickel based tubes are predominant, and some are amorphous.

The majority of the peaks in Fig. 2 match the known hydroxide and oxide phases of the respective metals but some oxides are detected. We specifically find the patterns expected for zinc hydroxide and oxide, malachite (Mg(OH)₂), copper hydroxide and oxide, hausmannite (Mn₃O₄), magnetite (Fe₃O₄) and goethite (FeO(OH)), nickel hydroxide and hydrated hydroxides, as well as β-Co(OH)₂. We are unable to provide a confident identification for the vanadyl-based samples. No indications of silicates or carbonates are found. We note that the characterization is in accord with Raman spectroscopy measurements (Fig. S1).

While in recent years considerable progress has occurred towards a theoretical description of the tube radius, the wall thickness, and certain oscillatory phenomena, the growth speed of precipitation tubes remains poorly understood.^{8,17} Possible factors that could affect the growth velocity include the solubility product and the zeta potential of the colloidal suspension. Beyond these equilibrium properties, the relative rates of the precipitation reaction, diffusion, and advective transport can also be expected to be important. Lastly, tube growth could be assisted by surface-mediated reactions at the tube rim. The complexity of these factors is clearly aggravated by the presence of numerous reaction species and complex polymerization processes and we therefore suggest that the chemically simplified reaction conditions of our experiment provide an ideal example for the investigation of growth speeds.

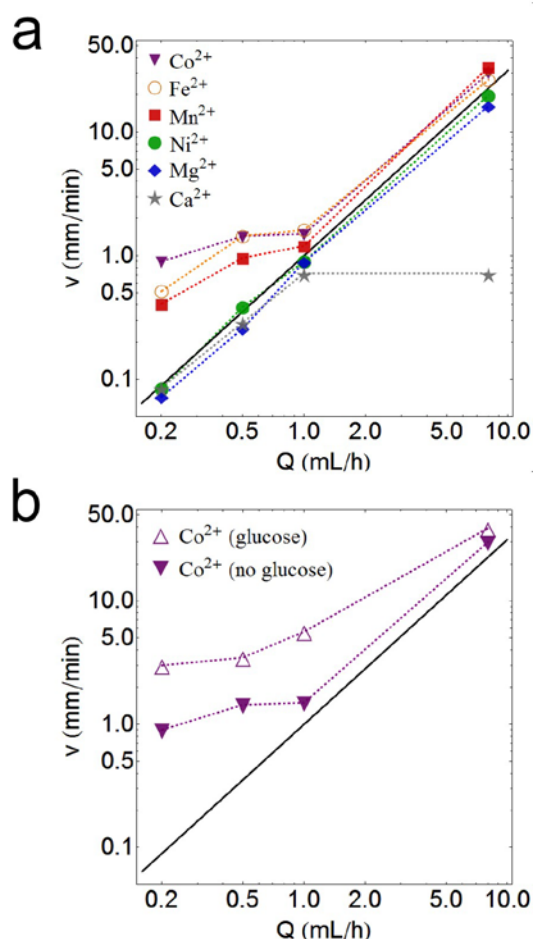


Fig 3. Double-logarithmic plots of the tubes' growth speed v as a function of the employed pump rate Q . The marker symbols distinguish between different metal chloride solutions (all 0.5 mol/L; see legend); dotted lines are only meant as a visual guide. The continuous black line has a slope of $3/2$. All measurements in (a) were performed without addition of glucose to the solution. Open triangles in (b) are obtained for $[\text{glucose}] = 0.5 \text{ mol/L}$. In both data sets (open, solid triangles) $[\text{CoCl}_2] = 0.5 \text{ mol/L}$.

In the following, we analyze these velocities for a wide range of pump rates Q and some additional parameter changes. Figure 3a shows the average growth speed for pump rates between 0.2 and 8.0 mL/h and for six different divalent metal solutions (see legend). Each velocity point is the average of at least two experiments in which the speed was measured as the rate of the tube's height increase. The latter analysis was performed by linear regression of height data spanning at least 2 but typically 5 cm. Notice that both axes are scaled logarithmically.

The growth speeds fall in the range of about 0.1 to nearly 40 mm/min, which is comparable to injection-controlled growth rates of tubes in silicate-containing systems.¹⁷ The speeds increase with increasing pump rates for essentially all tested solutions with the exception of CaCl_2 . This anomaly is most likely related to the solubility product of calcium hydroxide ($K_{\text{sp}} = 5.1 \times 10^{-6}$)¹⁸ which is four to five orders of magnitude higher than the solubility products of the other hydroxides investigated here. Clearly the comparatively

high solubility of Ca(OH)_2 is also responsible for the unusual fountain-like effects shown in Fig. 1h. Anomalies were also observed for tubes grown in CuCl_2 (see Fig. S2) and vanadyl solutions (see Fig. 1j). For the other solutions, we find that the growth speed increase according to the ordering: $\text{Ca}^{2+} < \text{Mg}^{2+} < \text{Ni}^{2+} \approx \text{Mn}^{2+} \approx \text{Co}^{2+} \approx \text{Fe}^{2+} (< \text{Cu}^{2+})$. At high pump rates, these differences correspond to velocity differences of more than 100% between Mg^{2+} and Mn^{2+} derived tubes.

Most importantly, the data in Fig. 3a reveal a power law dependence $v = k Q^\alpha$ between the growth speed and the pump rate with a power law exponent of $\alpha = 3/2$. In the double-logarithmic graph (Fig. 3a), the corresponding slope is represented by the continuous black line. At low flow rates we find deviations from this dependence for cobalt, iron, and manganese-based tubes. Notice that the corresponding metal chloride solutions have comparatively high densities (see Table S1). We hence suggest that these deviations are related to buoyancy effects that affect the physical characteristics of the reactant jet (and hence the tube growth) by shifting it away from a predominantly injection-speed controlled "pure jet" to a "lazy plume".¹⁹

To further evaluate the importance of density differences, we performed additional experiments in which the density of the outer reservoir solution is increased by addition of glucose (0.5 M). The results for the example of cobalt-based tube growth are shown in Fig. 3b. For comparison, the figure also regraphs the power law line for $\alpha = 3/2$ and the growth speed in glucose-free CoCl_2 solution. We find that an increase in density difference indeed increases the growth velocity and that the effect is strongest at low pump rates. This finding supports our hypothesis that the deviations from a simple power law result from buoyancy effects at low Q values.

The presence of a dominant power law $v = k Q^{3/2}$ in conjunction with our proposed explanation of deviations at low flow rates indicate that the tube growth dynamics is governed by hydrodynamic processes. However, the volume ratio $V_{\text{tube}}/V_{\text{injected}}$, which would equal 1 for tubes growing at the average fluid speed, is below 0.2 in many of our experiments (see Fig. S4). The results in Fig. 3a also show element-dependent offsets that correspond to differences in the proportionality constant k . These changes are likely related to the aforementioned physicochemical quantities such as the solubilities of the respective metal hydroxides. Clearly, more work is needed to elucidate these dependencies.

In conclusion, we have demonstrated that precipitation tubes can form in reactions between hydroxide and metal ion and that these simplified conditions reveal a scaling law for the growth velocity. Additional chemical species such as silicate, phosphate, borate, ammonia, and sulfide are not essential. This result suggests that in silicate-containing systems, silica precipitation is a secondary process with rather limited impact on the tubes' growth dynamics. Despite the name silica garden, silica would hence merely serve a density increasing and mechanically stabilizing role. In the context of closed-tube growth¹⁶, the silica-induced stabilization and effective elasticity changes are expected to be more important than for the open-tube growth investigated here.

We acknowledge financial support from the National Science Foundation (DMR-1005861). B.C.B. acknowledges the National Council for Scientific and Technological Development (CNPq, Brazil).

for a postdoctoral fellowship. We thank Bert van de Burgt for assistance with the Raman measurements.

Notes and references

- 1 S. Mann, *Biomining*, Oxford University Press, New York, **2001**.
- 2 (a) J. M. García-Ruiz, E. Melero-García, S. T. Hyde, *Science*, **2009**, **323**, 362-365; (b) W. L. Noorduin, A. Grinthal, L. Mahadevan, J. Aizenberg, *Science*, **2013**, **340**, 832-837; (c) B. A. Grzybowski, K. J. M. Bishop, C. J. Campbell, M. Fialkowski, S. K. Smoukov, *Soft Matter*, **2005**, **1**, 114-128; (d) I. R. Epstein, *Chem. Commun.*, **2014**, **50**, 10758-10767.
- 3 (a) N. Tompkins, N. Li, C. Girabawe, M. Heymann, G. B. Ermentrout, I. R. Epstein, S. Fraden, *Proc. Natl. Acad. Sci.*, **2014**, **111**, 4397-4402; (b) A. F. Taylor, M. R. Tinsley, *Nat. Chem.*, **2009**, **1**, 340-341.
- 4 (a) M. R. Tinsley, A. F. Taylor, Z. Huang, K. Showalter, *Phys. Chem. Chem. Phys.*, **2011**, **13**, 17802-17808; (b) M. R. Tinsley, D. Collison, K. Showalter, *J. Phys. Chem. A*, **2013**, **117**, 12719-12725.
- 5 (a) F. Haudin, J. H. E. Cartwright, F. Brau, A. De Wit, *Proc. Natl. Acad. Sci.*, **2014**, **111**, 17363-17367; (b) F. Haudin, V. Brasiliense, J. H. E. Cartwright, F. Brau, A. De Wit, *Phys. Chem. Chem. Phys.*, **2015**, **17**, 12804-12811; (c) I. Molnár, K. Kurin-Csörgei, M. Orbán, I. Szalai, *Chem. Commun.*, **2014**, **50**, 4158-4160; (d) B. Bohner, G. Schuszter, O. Berkesi, D. Horváth, A. Tóth, *Chem. Commun.*, **2014**, **50**, 4289-4291; (e) E. Tóth-Szeles, A. Tóth, D. Horváth, *Chem. Commun.*, **2014**, **50**, 5580-5582; (f) S. K. Smoukov, A. Bitner, C. J. Campbell, K. Kandere-Grzybowska, B. A. Grzybowski, *J. Am. Chem. Soc.*, **2005**, **127**, 17803-17807.
- 6 J. H. E. Cartwright, J. M. García-Ruiz, M. L. Novella, F. Otálora, *J. Colloid. Interf. Sci.*, **2002**, **256**, 351-359.
- 7 (a) J. H. E. Cartwright, B. Escribano, C. I. Sainz-Díaz, *Langmuir*, **2011**, **27**, 3286-3293; (b) J. Pantaleone, A. Toth, D. Horvath, J. R. McMahan, R. Smith, D. Butki, J. Braden, E. Mathews, H. Geri, J. Maselko, *Phys. Rev. E*, **2008**, **77**, 046207-1-12.
- 8 L. Roszol, O. Steinbock, *Phys. Chem. Chem. Phys.*, **2011**, **13**, 20100-20103.
- 9 (a) C. Ritchie, G. J. T. Cooper, Y. -F. Song, C. Streb, H. Yin, A. D. C. Parenty, D. A. Maclaren, L. Cronin, *Nat. Chem.*, **2009**, **1**, 47-52; (b) G. J. T. Cooper, R. W. Bowman, E. P. Magennis, F. Fernandez-Trillo, C. Alexander, M. J. Padgett, L. Cronin, *Angew. Chem. Int. Ed.*, **2012**, **51**, 12754-12758; (c) D. A. Stone, R. E. Goldstein, *Proc. Natl. Acad. Sci.*, **2004**, **101**, 11537-11541; (d) D. D. Double, A. Hellawell, *Nature*, **1976**, **261**, 486-488.
- 10 L. M. Barge *et al.*, *Chem. Rev.*, **2015**, Accepted: "From chemical gardens to chemobrionics".
- 11 (a) S. Thouvenel-Romans, J. J. Pagano, O. Steinbock, *Phys. Chem. Chem. Phys.*, **2005**, **7**, 2610-2615; (b) L. Roszol, R. Makki, O. Steinbock, *Chem. Commun.*, **2013**, **49**, 5736-5738; (c) B. C. Batista, P. Cruz, O. Steinbock, *ChemPhysChem*, **2015**, **16**, DOI: 10.1002/cphc.201500368.
- 12 J. J. Pagano, T. Bánsági Jr., O. Steinbock, *Angew. Chem. Int. Ed.*, **2008**, **47**, 9900-9903.
- 13 C. Collins, R. Mokaya, J. Klinowski, *Phys. Chem. Chem. Phys.*, **1999**, **1**, 4669-4672.
- 14 R. Makki, X. Ji, H. Mattoussi, O. Steinbock, *J. Am. Chem. Soc.*, **2014**, **136**, 6463-6469.
- 15 J. J. Pagano, S. Thouvenel-Romans, O. Steinbock, *Phys. Chem. Chem. Phys.*, **2007**, **9**, 110-116.
- 16 (a) R. E. Mielke, K. J. Robinson, L. M. White, S. E. McGlynn, K. McEachern, R. Bhartia, I. Kanik, M. J. Russell, *Astrobiology*, **2011**, **11**, 933-950; (b) L. M. Barge, I. J. Doloboff, L. M. White, G. D. Stucky, M. J. Russell, I. Kanik, *Langmuir*, **2012**, **28**, 3737-3721; (c) B. C. Batista, P. Cruz, O. Steinbock, *Langmuir*, **2014**, **30**, 9123-9129; (d) D. A. Stone, B. Lewellyn, J. C. Baygents, R. E. Goldstein, *Langmuir*, **2005**, **21**, 10916-10919; (e) V. Kaminker, J. Maselko, J. Pantaleone, *J. Chem. Phys.*, **2014**, **140**, 244901-1-7; (f) J. Maselko, M. Kiehl, J. Couture, A. Dyonizy, V. Kaminker, P. Nowak, J. Pantaleone, *Langmuir*, **2014**, **30**, 5726-5731; (g) M. Kiehl, V. Kaminker, J. Pantaleone, P. Nowak, A. Dyonizy, J. Maselko, *Chaos*, **2015**, **25**, 064310-1-8.
- 17 (a) S. Thouvenel-Romans, W. van Saarloos, O. Steinbock, *Europhys. Lett.*, **2004**, **67**, 42-48; (b) S. Thouvenel-Romans, O. Steinbock, *J. Am. Chem. Soc.*, **2003**, **125**, 4338-4341.
- 18 W. M. Haynes, T. J. Bruno, D. R. Lide, *CRC Handbook of Chemistry and Physics 96th Edition*, CRC Press, Boca Raton, **2015**.
- 19 R.-Q. Wang, A. Wing-Keung Law, E. E. Adams, O. B. Fringer, *Phys. Fluids*, **2009**, **21**, 125104-1-9.